Contributions of Bacterial Surface Polymers, Electrostatics, and Cell Elasticity to the Shape of AFM Force Curves

Stephanie B. Velegol† and Bruce E. Logan*

Department of Civil & Environmental Engineering, Penn State University, University Park, Pennsylvania 16802

Received December 17, 2001. In Final Form: April 1, 2002

Probing nanoscale interactions between an atomic force microscope tip and a bacterium may provide insight into the molecular level origins of bacterial adhesion. Distinguishing between the relevant surface interaction forces, such as steric and electrostatic interactions, is complicated by the elastic deformation of the bacterium. To probe the possible role of lipopolysaccharides (LPS) in bacterial adhesion and cell elasticity, atomic force microscopy (AFM) force images were obtained between a bare silicon nitride AFM tip and three different *Escherichia coli* K12 strains, each having a different length of LPS on their surface. Cell elasticity was varied with glutaraldehyde fixation. Bacterial force curves consisted of a nonlinear region 20−30 nm above the cell surface and a constant compliance (linear region) with a slope that was significantly less than that of a hard surface. AFM force curves obtained on the top of the cell were identical (linear and nonlinear regions) for all three strains, indicating a lack of a steric contribution of LPS to the force curve. Force images obtained off the center of the cell produced apparent long-range forces, but these were considered to be imaging artifacts produced by tip−surface geometries at the cell edges. Glutaraldehyde strongly affected the elasticity of the cell but did not affect the nonlinear portion of the force curve. The effective spring constant of the bacterium, calculated from the constant compliance region of the force curve, was found to increase 4-fold with the addition of 2.5% glutaraldehyde and was independent of the spring constant of the cantilever. The nonlinear portion of the curve is not consistent with electrostatic forces, because interaction distances were not a function of solution ionic strength. These results suggested that nonlinear forces were due to deformation of the bacterial surface layer.

Introduction

Bacterial adhesion is important in a variety of fields including bioremediation, biomaterial development, and marine biofouling. Although macroscopic properties of bacteria such as hydrophobicity and surface charge have been demonstrated to generally correlate with the extent of bacterial adhesion to a surface,[1,2] a molecular level understanding of the initial bioadhesion process is still lacking. Over the past few decades, force measurement techniques such as the surface force apparatus (SFA),[3,4] atomic force microscopy (AFM),[5] total interference reflectance microscopy (TIRM),[6,7] and differential electrophoresis[8] have made it possible to examine interactions between colloidal particles and surfaces. For example, using AFM, electrostatic interaction forces between a micron-sized colloidal probe, or the AFM tip itself, and a flat surface have been directly measured.[5] AFM has also been used to obtain topographic images of a variety of biological materials and cells, including bacteria, yeast, proteins, and DNA.

Although the interaction forces between a bacterium and a surface, such as an AFM tip or colloidal probe, can be directly measured by AFM force curve imaging,[9,10] the interpretation of the forces involved has been difficult. The main challenge in extracting tip−surface forces is that the bacterium deforms under an applied load so that the origin relative to the tip location is not known.[11] In the past, two approaches have been used to account for this deformation and to locate the surface relative to the tip. The first approach has been to ignore long-range surface forces and to assume that the interaction of the tip and the bacterium is purely due to deformation of the bacterium.[12−16] The inherent assumption for this approach is that the surface forces are too weak to deflect the cantilever. The second approach is to assume that the bacterium is linearly elastic and that all the nonlinearity displayed in force curves is a consequence of electrostatic and steric (electrosteric) surface forces.[9,10,17] Using this

* Corresponding author. Phone: 814-863-7908. Fax: 814-863-7304. Email: Blogan@psu.edu.

† Current address: Department of Chemical Engineering, Bucknell University, Lewisburg, PA 17837.

(1) van Loosdrecht, M. C. M.; Lyklema, J.; Norde, W.; Schraa, G.; Zehnder, A. J. B. *Appl. Environ. Microbiol.* **1987**, *53*, 1898−1901.

(2) van Loosdrecht, M. C. M.; Lyklema, J.; Norde, W.; Schraa, G.; Zehnder, A. J. B. *Appl. Environ. Microbiol.* **1987**, *53*, 1893−1897.

(3) Israelachvili, J.; Adams, G. E. *J. Chem. Soc., Faraday Trans.* **1978**, *74*, 975.

(4) Israelachvili, J. *Intermolecular & Surface Forces*; 2nd ed.; Academic Press: San Diego, 1992.

(5) Ducker, W. A.; Senden, T. J.; Pashley, R. M. *Nature* **1991**, *353*, 239−241.

(6) Prieve, D. C.; Luo, F.; Lanni, F. *Faraday Discuss. Chem. Soc.* **1987**, *83*, 297.

(7) Prieve, D. C. *Adv. Colloid Interface Sci.* **1999**, *82*, 93.

(8) Velegol, D.; Anderson, J. L.; Garoff, S. *Langmuir* **1996**, *12*, 4013−4110.

(9) Razatos, A.; Ong, Y.-L.; Sharma, M. M.; Georgiou, G. *Proc. Natl. Acad. Sci. U.S.A.* **1998**, *95*, 11059−11064.

(10) Camesano, T. A.; Logan, B. E. *Environ. Sci. Technol.* **2000**, *34*, 3354−3362.

(11) Chan, D. Y. C.; Dagastine, R. R.; White, L. R. *J. Colloid Interface Sci.* **2001**, *236*, 141.

(12) Hoh, J. H.; Schoenenberger, C.-A. *J. Cell Sci.* **1994**, *107*, 1105−1114.

(13) A-Hassan, E.; Hienz, W. F.; Antonik, M. D.; D'Costa, N. P.; Nageswaran, S.; Schoenenberger, C.-A.; Hoh, J. H. *Biophys. J.* **1998**, *74*, 1564−1578.

(14) Arnoldi, M.; Fritz, M.; Bauerlein, E.; Radmacher, M.; Sackmann, E.; Boulbitch, A. *Phys. Rev. E* **2000**, *62*, 1034−1044.

(15) Arnoldi, M.; Kacher, C. M.; Bauerlein, E.; Radmacher, M.; Fritz, M. *Appl. Phys. A* **1998**, *66*, S613−S617.

(16) Braet, F.; Rotsch, C.; Wisse, E.; Radmacher, M. *Appl. Phys. A* **1998**, *66*, S575−S578.

10.1021/la011818g CCC: $22.00
Published on Web 05/23/2002

second approach, Camesano and Logan[10] investigated the interactions between a silicon nitride tip and a bacterium (*Pseudomonas putida* KT2442). They concluded that the repulsive forces that were measured, which extended over hundreds of nanometers, were due to electrosteric repulsion by lipopolysaccharides (LPS) and extracellular polymer substances (EPS) on the bacterial surface.[10]

To study the role of the LPS molecules on adhesion, Razatos et al.[9] measured forces between various surfaces and a monolayer of *Escherichia coli* bonded to the AFM tip. Different *E. coli* strains were used that were genetically modified to have different lengths of their LPS layers. They observed that the electrostatic repulsive interaction decreased as the LPS was progressively truncated. Thus, they concluded that bioadhesion would increase with the length of the LPS. There were two important limitations of their approach. First, AFM experiments were performed using only glutaraldehyde-treated bacteria to minimize bacterial deformation. Second, force curves were obtained randomly on the bacterial lawn so that the exact location of the tip on a bacterial surface was not known.

The contribution of the LPS layer to bacterium−surface interactions remains unresolved by these studies due to an insufficient consideration of cell elasticity in concert with other complicating factors such as electrostatics, the effects of glutaraldehyde on cell adhesion properties, and the analysis of force curves obtained at random locations on bacterial surfaces. To further examine these interactions, we measured the force curves on glutaraldehyde-free *E. coli* strains having genetically modified LPS. We used a defined force analysis procedure to find a center location on the top of a bacterium to ensure an exact and reproducible tip−bacterium interaction. We demonstrated that if LPS or electrostatic repulsion produces interactions between the tip and the bacterium, they could not be captured using current AFM force imaging techniques. As a part of this analysis, we showed that glutaraldehyde fixation reduces bacterial elasticity and speculated on the origin of the forces that produce nonlinear deflection of the cantilever when the AFM tip was near or on bacterial surfaces.

Methods

Bacteria. Three different *E. coli* K12 mutant strains with different LPS compositions were used in the experiments.[9,18] The parent strain (D21) contained the KDO and inner and outer core but no O-antigen, while the mutated strain D21f2 contained only the KDO. *E. coli* K12 strain JM109 contained the KDO and the inner and outer core, as well as the full O-antigen strain. D21 and D21f2 were obtained from the *E. coli* Genetic Stock Center at Yale University, and JM109 was obtained from Shahriar Mobashery at Wayne State University.

Bacteria were grown in Luria broth Millers at 37 °C and harvested during mid-log-growth at a cell concentration of $\sim 10^8$ mL^{-1}. For glutaraldehyde-free solutions, the bacteria were washed once in a phosphate buffer solution (PBS) and then twice in 1 mM Tris buffer by centrifugation (2800*g*). For solutions containing glutaraldehyde, bacteria were rinsed and resuspended twice in PBS buffer, incubated with glutaraldehyde (final concentration of 2.5%) at 20 °C for 2 h, rinsed twice, and resuspended in 1 mM Tris. Glutaraldehyde (50%, Sigma) was stored at −70 °C and thawed 5 min before use to prevent polymerization.[19]

Thin glass cover slides (24 × 60 mm) were cleaned by soaking in aquaregina (3:1 HCl/H_2NO_3) overnight, rinsing copiously with Milli Q water, soaking in piranha solution (4:1 H_2SO_4/H_2O_2) for 2 h, and rinsing again with Milli Q water. Slides were stored in Milli Q water.

To image bacteria with AFM, the bacteria must be tightly bound to the glass surface.[10] Poly(ethyleneimide) (PEI; Aldrich, 750 000 Da) was used to create a positively charged glass surface that promoted irreversible adhesion of the bacteria.[20] To prepare slides, the PEI solution (0.2%, 1 mL) was placed on the glass slide for 3−5 h and then rinsed with Milli Q water. A bacterial suspension (1 mL) was placed on the slide, and after 1 h the bacteria-coated slide was rinsed and stored in the experimental solution (usually 1 mM Tris) for use later that same day. This procedure resulted in a surface coverage of 25−30% (by area).[21] Using a concentration of bacteria greater than 10^8 mL^{-1} resulted in a higher surface coverage that was difficult to image with AFM. The bacteria-coated slide was removed from solution, and the bottom of the slide was dried with N_2. The top of the slide containing attached bacteria was never dried before imaging.

Zeta potential measurements on bacteria were obtained using a Zeta-Pals Instrument (Brookhaven).

Atomic Force Microscopy. All AFM experiments were performed with a BioScope AFM (Digital Instruments) that consists of an AFM head mounted on an inverted microscope. In this system, the sample remains stationary on the microscope platform while the cantilever and tip are moved by the piezo. All samples were imaged in aqueous solutions using a fluid cantilever holder (unless stated otherwise). The solutions used were either 1 mM Tris ($pK_a = 8.3$) or 1 mM Tris with 100 mM NaCl. The DNP-S silicon nitride cantilevers (Digital Instruments) had a force constant of either 0.045 N/m (long/thin tip) or 0.25 N/m (short/fat tip) as measured by the Cleveland method.[22] All tips were cleaned in a BioForce UV/ozone cleaner before use.

Bacteria were located and imaged using tapping mode to minimize contact of the tip with the cells. Images were obtained in liquid at a drive frequency of ∼8 kHz and a drive amplitude of 300 mV. Only bacteria with a height greater than 750 nm were chosen for force curve analysis. Imaging one bacterium multiple times usually did not alter the image (unless otherwise stated).

All force curves were obtained in contact mode. To obtain a force curve, one area of a bacterium was selected from the tapping mode image and the cantilever was withdrawn 10 μm. The AFM tip was then lowered manually by the piezo to the surface in 1 μm increments until deflection of the cantilever was observed. The scan size and frequency were set at 1 μm and 1 Hz, respectively, during force imaging. Multiple force curves were obtained around and on the bacterium to ensure that the force curve represented the interaction between the tip and the top of the bacterium. Multiple force curves were also obtained on the PEI-coated silica surface around each bacterium. When changing the horizontal position of the tip over the bacterium, the tip was first completely retracted from the surface. No difference was observed in the force curve between an AFM tip and a glass slide and an AFM tip and a PEI-coated glass slide as shown below. The slope of the constant compliance region of the force curves obtained on the PEI-coated glass slide was used to convert the deflection in millivolts to nanometers.

Calculation of Electrostatic Force between Tip and Bacterium. To model the electrostatic and van der Waals forces, both the AFM tip and the bacterium were modeled as spheres.[24] The electrostatic and van der Waals interaction energies between two spheres with constant surface potential are given, respectively, as

$$\phi_{ES}(h) = \pi\epsilon\left(\frac{a_t a_b}{a_t + a_b}\right)\left[2\psi_t\psi_b \ln\left(\frac{1 + e^{-\kappa h}}{1 - e^{-\kappa h}}\right) + (\psi_t^2 + \psi_b^2)\ln(1 - e^{-2\kappa h})\right] \quad (1)$$

(17) Ong, Y.-L.; Razatos, A.; Georgiou, G.; Sharma, M. M. *Langmuir* **1999**, *15*, 2719−2725.
(18) Burks, G.; Velegol, S. B.; Logan, B. E. Manuscript in preparation.
(19) Hopwood, D. *Histochem. J.* **1972**, *4*, 267−303.
(20) D'Souza, S. F.; Melo, J. S.; Deshpande, A.; Nadkarni, G. B. *Biotechol. Lett.* **1986**, *8*, 643−648.
(21) Pardi, S.; Logan, B. E. Manuscript in preparation.
(22) Cleveland, J. P.; Manne, S.; Bocek, D.; Hansma, P. K. *Rev. Sci. Instrum.* **1993**, *64*, 403−405.

$$\phi_{vdw}(h) = -\frac{A}{6h}\left(\frac{a_t a_b}{a_t + a_b}\right) \quad (2)$$

where h is the separation distance, ψ_t and ψ_b are the surface potentials, a_t and a_b are the radii of the tip and bacterium, respectively, κ is the inverse Debye length, ϵ is the permittivity of water, and A is the Hamaker constant.[23] The total force is calculated by differentiating the energy with respect to separation distance:

$$F(h) = \frac{a_t a_b}{a_t + a_b}\left\{2\pi\epsilon\kappa e^{-\kappa h}\left(\frac{\psi_t^2 e^{-\kappa h} + \psi_b^2 e^{-\kappa h} - 2\psi_t\psi_b}{e^{-2\kappa h} - 1}\right) - \frac{A}{6h^2}\right\} \quad (3)$$

The AFM tip was modeled as a sphere with a radius of 250 nm, and an average radius of 500 nm was used for all bacteria. Although the nominal tip radius of curvature is 5−40 nm (from www.di.com), Senden and Drummond[24] have shown that a larger tip radius is needed to resolve electrostatic models based on a sphere with pyramid-shaped AFM tips and surfaces. The ionic strength of 1 mM Tris at pH 9 was calculated to be 0.15 mM, resulting in a Debye length of 26 nm. Table 1 shows the zeta potentials of the three bacteria used in this study in 1 mM Tris. In the pH range here (8−9), the silicon nitride tip was negatively charged and should have zeta potentials that range from −40 to −90 mV.[24] The surface potential of both the tip and the bacterium were assumed to be equal to the measured zeta potential. A Hamaker constant of 10^{-20} J was chosen, consistent with others.[10]

Results

Images. *E. coli* bacteria were imaged both in the presence and absence of glutaraldehyde. There were no differences in the size, morphology, or clarity of images of the three strains of *E. coli* in the absence of glutaraldehyde. The addition of glutaraldehyde did not change the dimensions of the bacterium but did produce clearer images. Bacteria were typically 1 μm wide and 3 μm long, consistent with the known dimensions on *E. coli* (Figure 1). Images obtained from the change in piezo position (height images) indicated that the height of the bacteria ranged from 0.75 to 1.2 μm.

The apparent "shadow" associated with the cell, shown on the upper and right sides of the bacterium in Figure 1, results from the relatively large height of a bacterium and the pyramid geometry of the AFM tip. Shadows in AFM images have been observed by others (Bolshakova et al.;[25] see their Figure 1b) when imaging relatively isolated *E. coli* cells in water. When the bacteria were imaged in air over larger distances, these shadows disappeared (Figure 2a). Such shadows were also not present when imaging cells having a reduced height in water or cells that appeared "deflated" (Figure 2b).

Effect of LPS on Force Curves. The differences in the LPS length of the D21 and D21f2 strains did not result in any measurable differences in the shape of the AFM force curve (Figure 3). Identical force curves to those shown in Figure 3 were also obtained for JM109, which contains the O-antigen and therefore has the longest LPS molecule of the three strains, and for bacteria treated with 2.5% glutaraldehyde (data not shown). A force curve for a bare AFM tip on a PEI-coated silica surface, also shown in Figure 3, was not significantly different from a force curve obtained on a cleaned glass surface.

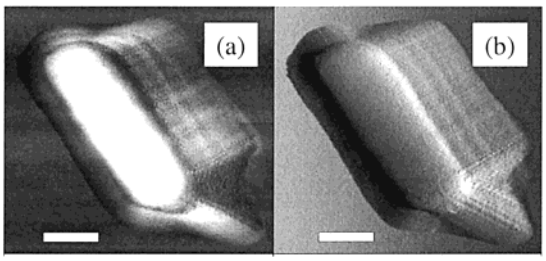

Figure 1. Typical tapping mode phase (a) and amplitude (b) image of K12 *E. coli* in the absence of glutaradehyde. The length and width of the bacterium are 3.4 μm and 1.1 μm, respectively. The white bar on the images represents 1 μm.

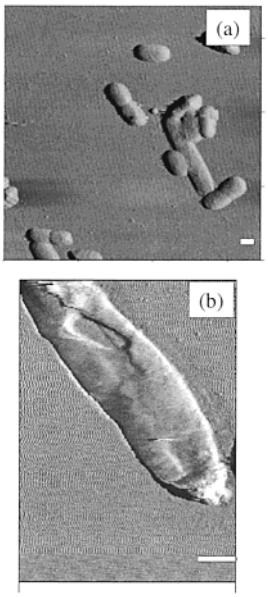

Figure 2. (a) Several *E. coli* imaged in air and (b) a single, deflated *E. coli* imaged in water (amplitude mode). In both cases, the shape of the bacterium appears normal due to the reduced height of the cells when being imaged. The white bar indicates 1 μm.

Table 1. Zeta Potential Measurements of D21, D21f2, and JM109 in 1 mM Tris before and after 2.5% Glutaraldehyde Treatment

	zeta potential, mV	
	no glutaraldehyde	2.5% glutaraldehyde
D21	40 ± 3	41 ± 3
D21f2	43 ± 3	43 ± 5
JM109	50 ± 1	50 ± 2

The force curves for the two bacteria in Figure 3 contain both a linear and a nonlinear region. The dotted line in Figure 3, representing the extension of the *linear* region, has a slope of approximately −0.52 nm/nm. For the PEI-coated silica surface, the slope of the linear region is equal to −1 nm/nm. The intersection of both these linear lines with the *x*-axis was used to define the origin for the piezo position. On the basis of this origin, the nonlinear portion of the force curve extends from approximately −20 to +20 nm in the piezo position.

Analysis of the Linear Slope of the Force Curve. The slope of the linear portion of the force curve to the left of the origin (see Figure 3), or constant compliance, can be used to calculate the spring constant of the bacterium assuming that deflection of the cantilever is only due to elastic deformation of the bacterium.[14] This calculation requires that we define the distances that the tip and bacterium deflect during force imaging. Because

(23) Russel, W. B.; Saville, D. A.; Schowalter, W. R. *Colloidal Dispersions*; Cambridge University Press: Cambridge, 1989.

(24) Senden, T. J.; Drummond, C. J. *Colloids Surf., A* **1995**, *94*, 29−51.

(25) Bolshakova, A. V.; Kiselyova, O. I.; Filonov, A. S.; Frolova, O. Yu.; Lyubchenko, Y. L.; Yaminsky, I. V. *Ultramicroscopy* **2001**, *86*, 121−128.

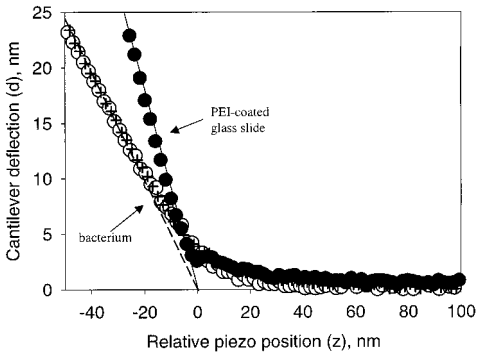

Figure 3. Deflection of the cantilever vs piezo movement for the interaction of a silicon nitride tip and D21 (open circles) and D21f2 (crosshair) bacteria and a PEI-coated glass slide (filled circles). The force curves for the three bacteria overlap, showing that the LPS contributes to neither the linear nor the nonlinear response. The extension of the linear fit to the data (dotted lines) to the *x*-axis defines the zero position of the piezo position.

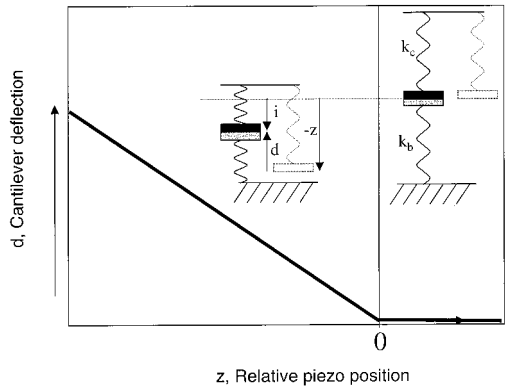

Figure 4. Schematic diagram representing an AFM cantilever with a spring constant k_c and a deformable surface with a spring constant k_b assuming linear deformation of the bacterium and no nonlinear interactions between the tip and the bacterium. On the right side of the figure, the two surfaces just make contact but no compression has occurred and the piezo position is defined as zero. As the piezo moves a distance of *z* in the negative direction, the cantilever (upper) spring compresses a distance of *d* and the bacterium (lower) spring compresses by *i*.

both the bacterium and the cantilever can be modeled as springs, as shown in Figure 4, both the tip and the bacterium can move during force imaging. The bottom of the lower spring (bacterium) is fixed in space, while the top of the upper spring (cantilever) moves due to the piezo movement. This initial approach is depicted in Figure 4 (right side), where it can be seen that the springs have just made contact but neither spring is compressed. As the piezo moves a distance *z* in the negative direction, both springs compress as shown in Figure 4 (left side). The compression distances of the cantilever spring, *d*, and the bacterium spring, *i*, are measured from the bottom of the uncompressed spring to the bottom of the compressed spring. The length of the uncompressed cantilever spring is shown by the dotted spring in Figure 4, while the length of the uncompressed bacterium spring is equal to the distance between the bottom surface and the dotted horizontal line.

The distance that the piezo has moved, *z*, is defined as zero where the springs first make contact and becomes negative as the springs compress (see Figure 4). The force, *F*, at any piezo position, *z*, can be calculated as

$$F(z) = k_c d = k_b i \tag{4}$$

where k_c and k_b are the spring constants of the cantilever and the bacterium, respectively. For two linear springs in contact, the magnitude of the piezo movement is equal to the sum of the compression of the two springs, or

$$-z = d + i \tag{5}$$

Since the value of the linear slope, *s*, is the ratio of *d* to *z*, combining eqs 4 and 5 gives

$$k_b = -k_c \frac{s}{1+s} \tag{6}$$

The spring constant of the bacterium can therefore be directly calculated using eq 6. When imaging a hard surface with an essentially infinite spring constant, such as a glass slide, $s = -1$.

In the absence of glutaraldehyde, the spring constant of the bacterium was calculated to be 0.040 ± 0.005 N/m (Table 2), a value that is independent of the spring constant of the cantilever. For example, increasing the spring constant of the cantilever (k_c) from 0.045 to 0.25 N/m decreased the slope, on average, from -0.48 ± 0.10 to -0.13 ± 0.04 (see Figure 5 for one example and Table 2 for the average of multiple force curves). The spring constant of the bacterium ($k_b = 0.044 \pm 0.014$ N/m) calculated using a cantilever with a spring constant of $k_c = 0.045$ N/m, was not statistically different from that measured using a stiffer cantilever with a much higher spring constant of $k_c = 0.25$ N/m ($k_b = 0.037 \pm 0.014$ N/m). Thus, using a stiffer cantilever increased the indentation of the cantilever, potentially making AFM measurements more destructive, but did not change the spring constant of the bacterium.

Adding glutaraldehyde stiffened the bacterium but did not make it as rigid as a glass surface (Figure 6). In the presence of 2.5% glutaraldehyde, the average slope of the constant compliance region was $s = -0.75$ nm/nm for $k_c = 0.045$ N/m and $s = -0.43$ nm/nm for $k_c = 0.25$ N/m. These slopes indicated that glutaraldehyde treatment increased the bacterium spring constant by a factor of 3−5 (Table 2).

Evaluation of the Nonlinear Portion of the Force Curve. The presence of a nonlinear region of the force curve makes the analysis of the two springs more complicated than that described previously in Figure 4. These nonlinear responses must be due to either (1) electrostatic and van der Waals forces, (2) steric forces due to EPS, or (3) nonlinear deformation of the bacterium. The nonlinearity is not due to the presence of LPS since it was found that the length of the LPS did not affect the nonlinear portion of the curve (see Figure 3).

The electrostatic and van der Waals forces between the tip and surface can be modeled if the separation distance (*h*) between the AFM tip and the bacterium is known. To calculate this distance, both the tip and the surface were modeled as perfectly elastic springs having charged surfaces that produced a nonlinear force between the two surfaces (Figure 7). The distance between the springs at any piezo position, *z*, can be calculated as

$$h = z + i + d = z + d\left(\frac{k_c + k_b}{k_c}\right)$$

where the distances used in this equation are shown for a generalized force curve in the bottom of Figure 7.

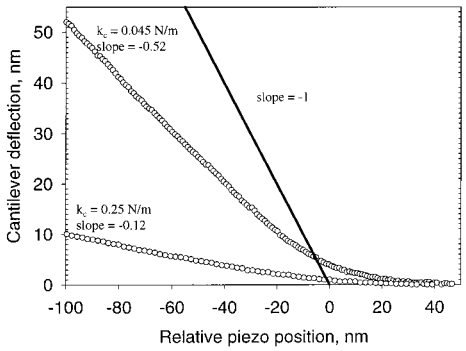

Figure 5. Cantilever deflection vs relative piezo position during the interaction between two silicon nitride AFM tips ($k_c = 0.045$ and 0.25 N/m) and the bacterium. The increase in the spring constant of the cantilever decreases the slope but does not change the calculated spring constant of the bacterium.

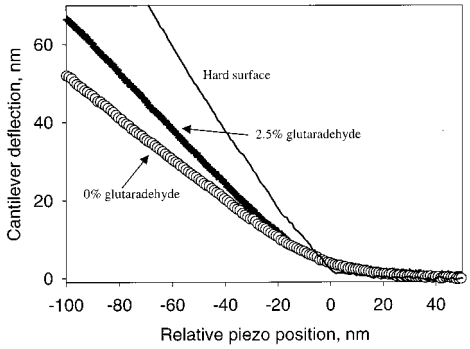

Figure 6. Cantilever deflection vs relative piezo position during the interaction between a silicon nitride AFM tip and the bacterium with 0% glutaraldehyde, the bacterium with 2.5% glutaraldehyde, and a PEI-coated slide. Adding 2.5% glutaraldehyde stiffens the cell and increases the linear slope but does not cause the bacterium to become infinitely stiff. (See Table 2 for a summary of the slopes and spring constants calculated.)

The distances described above are shown graphically in Figure 7. As the tip approaches the surface (point a), there is no deflection of the cantilever up to a distance z, where the separation distance (h_a) and piezo distance from the origin, z_a, are the same. As the tip moves nearer to the surface, long-range interactions (e.g., electrostatics) cause both the tip and the surface to deflect a distance of d_b and i_b, respectively. At position b, the bacterium surface is no longer located at the origin ($z = 0$) because it has been pushed down; the bacterial surface is now a distance $h_b = z_b + i_b + d_b$ from the tip. Position c is defined as the origin ($z = 0$), because this is the point where the tip and bacterium would have made contact in the absence of electrostatic repulsion. However, electrostatic repulsion causes the tip and the bacterium to be separated by a distance equal to h_c. As the piezo continues to move down (position c to position d in the force curve), the total force applied to the cantilever continues to increase and now is sufficient to move the tip and bacterial surface closer to each other. By point d, the force applied to the tip is large enough to have completely overcome electrostatic repulsion, and the tip and bacterium finally come into contact. As the piezo moves down past point d, the distance between the two springs (the bacterium and the tip) is equal to zero, and both springs compress linearly with the piezo position. The dashed line in Figure 7 represents the linear interaction of the tip and the bacterium in the absence of nonlinear (electrostatic) interactions (see Figure 4).

The deflection of the cantilever as a function of piezo position for D21 in Figure 2 was converted to a deflection

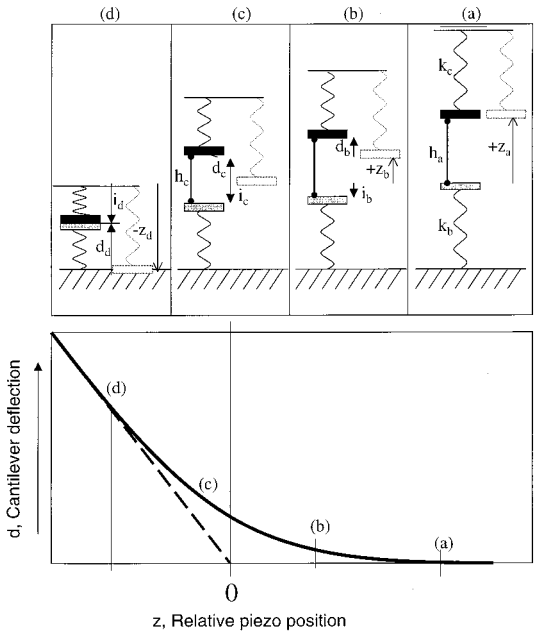

Figure 7. Schematic diagram of the interaction and separation distance, h, between the AFM tip and a deformable bacterium in the presence of electrostatic repulsion. Both the AFM cantilever and the bacterium surface are modeled as elastic springs, and the piezo position, z, is equal to zero in (c). At (a), the tip and the bacterium are not interacting. At (b), the tip and the bacterium compress due to repulsive interaction but are not touching. At (c), where the uncompressed springs would have made contact in the absence of electrostatic repulsion, the piezo position is defined as zero. At (d), both the tip and bacterium come into contact and compress linearly with a change in the piezo position.

versus separation distance plot and compared to the theoretical prediction from eq 3 for ψ_t equal to either −45 or −85 mV (Figure 8) to test if electrostatic interactions can explain the nonlinearity observed in the force curve in Figure 7 between points a and d. The cantilever began to measurably deflect at a separation distance of 40 nm and deflected up to 8 nm at small separation distances. The model predicted a measurable deflection (>0.5 nm) at a piezo position of 50−70 nm, and the maximum calculated deflection due to electrostatic repulsion and van der Waals attraction was 2 nm. The predicted repulsive interactions from eq 3 increased when the value of the zeta potential of the tip increased from −45 to −85 mV.

If the nonlinear region in the force curve was due to electrostatic forces, the size of this nonlinear region should have decreased when ionic strength was increased. However, increasing the ionic strength had very little effect on the interaction between the tip and the bacterium. In fact, increasing the ionic strength caused the interaction distance to stay the same or to increase (data not shown), indicating that electrostatic forces between the tip and bacterium were not directly responsible for the nonlinear portion of the force curve.

The size of the nonlinear region in the force curve also depended on both the position of the tip over the bacterium and the height of the bacterium. An increase in the nonlinear response was observed as the tip moved from the top of a bacterium to the side of the bacterium (Figure 9). This was speculated to be due to interactions between the side of the bacterium and the side of the AFM tip.[15] A similar increase in the apparent range of nonlinear forces was observed for bacteria that were deflated, or likely killed, during attachment to the surface (Figure 10).

Table 2. Slope of the Linear Region, *s*, and Calculated Spring Constant of the Bacteria, k_b, for Two Different Cantilever Spring Constants, k_c

	s, nm/nm		k_b, N/m	
k_c, N/m	no glutaraldehyde	2.5% glutaraldehyde	no glutaraldehyde	2.5% glutaraldehyde
0.045	0.48 ± 0.10	0.75 ± 0.01	0.044 ± 0.014	0.13 ± 0.01
0.250	0.13 ± 0.04	0.43 ± 0.02	0.037 ± 0.014	0.19 ± 0.02

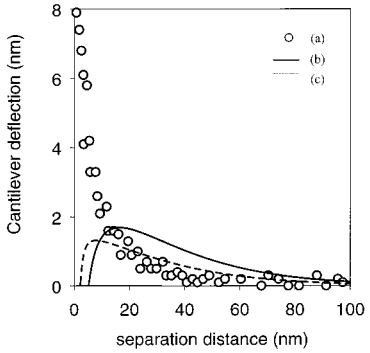

Figure 8. Deflection of the cantilever vs separation distance for the interaction of a silicon nitride tip and D21 (a). A model for the electrostatic repulsion and van der Waals attraction between the tip and the bacterium for $\psi_t = -45$ mV (b) and $\psi_t = -85$ mV (c).

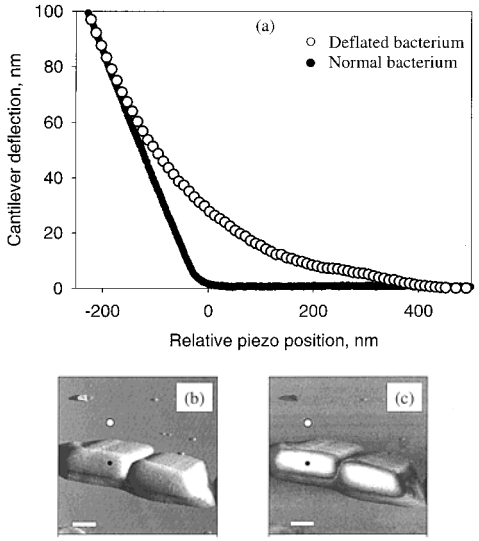

Figure 9. (a) Cantilever deflection vs relative piezo position during the interaction between an AFM tip and two locations on a JM109 bacterium. (b) Tapping mode amplitude (b) and phase (c) image of the bacterium. The positions of the filled and empty circles on the images correspond to the force curves in (a). The white bar on the images represents 1 μm.

Compared to those of fully inflated bacteria, these force curves show a lower slope and more nonlinearity suggesting nonlinear elasticity effects.

Discussion

The spring constant of *E. coli* bacteria reported in Table 2 compares favorably to spring constants of many other microorganisms that have been measured. For example, Arnoldi et al. reported effective spring constants of 0.042 N/m for *Magnetospirillum gryphiswaldense* (DSM6361) independent of sucrose concentration.[15] Hoh and Schoenenberger reported spring constants that ranged up to 0.015 N/m for Madin−Darby canine kidney cells.[12] Others have also found that glutaraldehyde, which increases the stiffness of biological cells by cross-linking proteins and amino acids within the peptidoglycan layer, increases the

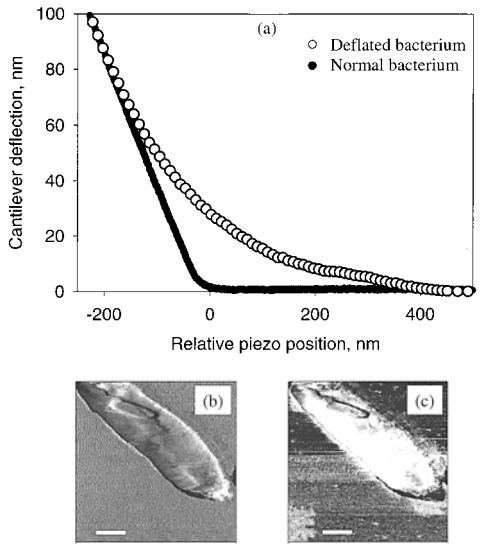

Figure 10. (a) Cantilever deflection vs relative piezo position during the interaction between an AFM tip and a normal JM109 bacterium and a deflated JM109 bacterium. (b) Tapping mode amplitude (b) and phase (c) image of the deflated bacterium. The height of the deflated bacterium was less than 200 nm. The white bar on the images represents 1 μm.

spring constant.[19] Cross-linking occurs within minutes following the addition of glutaraldehyde to cells[12] and increases the modulus of elasticity of liver endothelial cells from 1 kPa to over 100 kPa.[16]

In contrast to the work presented here, Ong et al. previously found that the addition of 2.5% glutaraldehyde caused *E. coli* to be infinitely stiff and they reported that the composition of the LPS changed the interaction energy between an AFM tip and glutaraldehyde-treated *E. coli*.[17] They also reported that the interaction energy changed from repulsive to attractive as the LPS length increased from D21f2 to D21. Since the repulsive interaction decreased with ionic strength, they claimed that repulsive interactions were due to electrostatic repulsion. In our experiments, no change in the interaction forces between D21 and D21f2 was observed even though our procedure was nearly identical to that of Ong et al.[17]

There are a few possible explanations for the discrepancy between our work and that of Ong et al.[17] Most of their work was done with bacteria attached to an AFM tip, and under these conditions the exact position of the bacterium on the tip is not known. Although they reported they found similar results for the interaction between a bare silicon nitride tip and a lawn of bacteria,[9] they did not image the bacterium first before obtaining a force curve to ascertain the exact location of the tip on the bacterium. As we have shown here, a force curve on a bacterium is sensitive to the location of the tip over the bacterium. A tip that is not centered over the bacterium can produce nonreproducible and apparent long-range forces. Furthermore, their scanning electron microscope images of the bacterial lawn showed a monolayer of bacteria, either on the tip or on the surface. This crowding may have produced different interaction forces. In our experiments, bacteria were imaged only when they were well isolated from one

another. Finally, although the same buffer was used in both experiments (1 mM Tris), the pH measured in our system was 8−9 while theirs was 7.5. This increase in the pH would increase the charge of the AFM tip and may have screened any attractive forces.

Recent macroscopic bioadhesion measurements have demonstrated that D21 has a *lower* sticking coefficient than D21f2 and that cell adhesion increases in the presence of 2.5% glutaraldehyde.[18] These macroscopic measurements do not support the previous AFM predictions of Ong et al.[17] and Razatos et al.[9] that D21 would have a *higher* sticking coefficient than D21f2 due to the measured attractive interactions or that glutaraldehyde would not affect adhesion.

Origin of Nonlinear Forces. There are reasons other than the LPS and electrostatic forces that can produce nonlinear interactions between an AFM tip and a bacterium. One possibility is that the nonlinear response is due to the presence of EPS on the surface of the bacterium. Camesano and Logan[10] found that nonlinear forces were measured at hundreds of nanometers from the surface of *Burkholderia cepacia* G4 and *P. putida* KT2442. Their models suggested that extracellular polymers reached lengths ranging from 230 to 1040 nm. In the experiments presented here, however, the nonlinear distances were much smaller, reaching overall distances of less than 50 nm. While this could indicate that the EPS, if present on the bacterium, were much smaller in length than those measured by Camesano and Logan, EPS would fail to account for the nonlinearity observed on the side of the bacterium or on a deflated bacterium.

Nonlinearity due to viscoelasticity of biological cells can be determined by changing the speed, or frequency, of the tip/bacterium interaction. Peterson et al.[26] and Hoh and Schoenenberger[12] observed changes in the response of fibroplasts and MDCK cells, respectively, with a change in scan frequency. A-Hassan et al. reported that force curves collected at scan rates below 0.5 μm/s will be dominated by an elastic response.[13] In our experiments, however, no changes in the force curve were observed when the frequency was varied from 0.1 to 30 Hz (0.1−30 μm/s).

On the basis of the force curves obtained here, we speculate that the nonlinear region was due to a variation in the cell elasticity during the initial penetration of the AFM tip into the outer surface layer of the bacterium. The peptidoglycan layer confers most of the rigidity of a bacterium. In Gram-negative bacteria, such as *E. coli*, the peptidoglycan layer is buried beneath the outer membrane in the periplasm at a depth of 8−23 nm. Thus, it may be that nonlinear deformation dominates during the initial penetration until the contact of the tip with the peptidoglycan layer. This model would explain our consistent force curves even in the absence of the length of the LPS on the outer surface. A varying elastic modulus of the bacterium outer layer might also explain why we observe a variation in the nonlinearity for a deflated bacterium and for interactions with the side of the bacterium as the peptidoglycan layer under such conditions would not directly be probed by the AFM tip.

Nonlinearity has previously been found to be a function of indentation depth and thickness for both biological cells and polymers. For example, Hoh and Schoenenberger reported that the spring constant of a Madin−Darby canine kidney cell changed from 0.002 to 0.015 N/m as the indentation depth increased from 1 to 2 μm.[12] When the cells were stiffened by the addition of glutaraldehyde in situ, the nonlinear distance decreased. Domke and Radmacher observed an increase in the apparent Young's modulus as the thickness of the gelatin film decreased.[27] Thus, the strongest evidence at this time is that nonlinear forces measured for bacteria are due to nonlinear elasticity from the molecular layers on bacteria.

Acknowledgment. This research was supported by the National Science Foundation (NFS) CRAEMS program (Grant CHE-0089156). The AFM used in this research was partially funded by the Penn State Biogeochemical Research Initiative for Education (BRIE) (NSF IGERT Grant DGE-9972759). The authors thank D. Velegol, J. Feick, and T. Matsoukas for providing the electrophoretic mobility data.

LA011818G

(26) Peterson, N. O.; McConnaughey, W. B.; Elson, E. T. *Proc. Natl. Acad. Sci. U.S.A.* **1982**, *79*, 5327−5331.

(27) Domke, J.; Dannohl, S.; Parak, W. J.; Muller, O.; Aicher, W. K.; Radmacher, M. *Colloids Surf. B* **2000**, *19*, 367−379.